Supporting Information

Sequential Effects of Two Cations on the Fluorescence Emission of a Coordination Polymer with Zn_4O Core in Node

Jagajiban Sendh, and Jubaraj B. Baruah*

Department of Chemistry, Indian Institute of Technology Guwahati, Guwahati-781039, Assam, India.

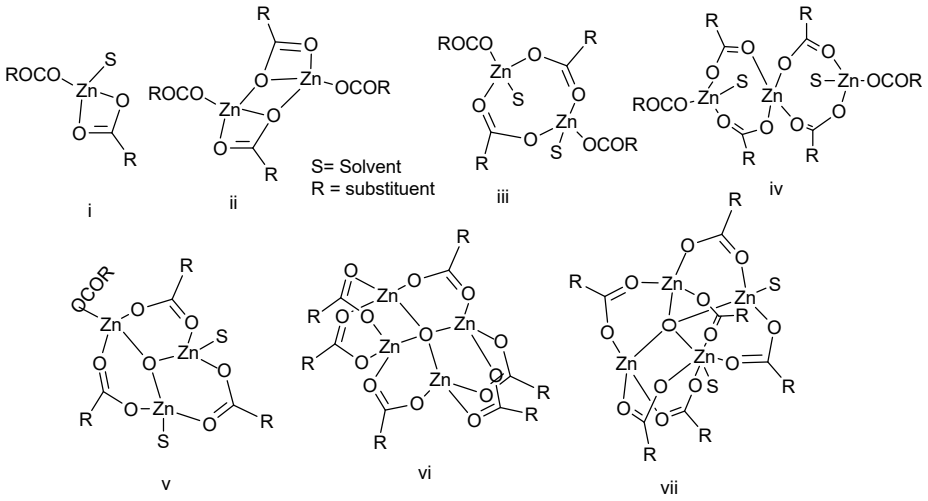

Figure S1: Illustrations of some nodes of zinc carboxylate coordination polymers

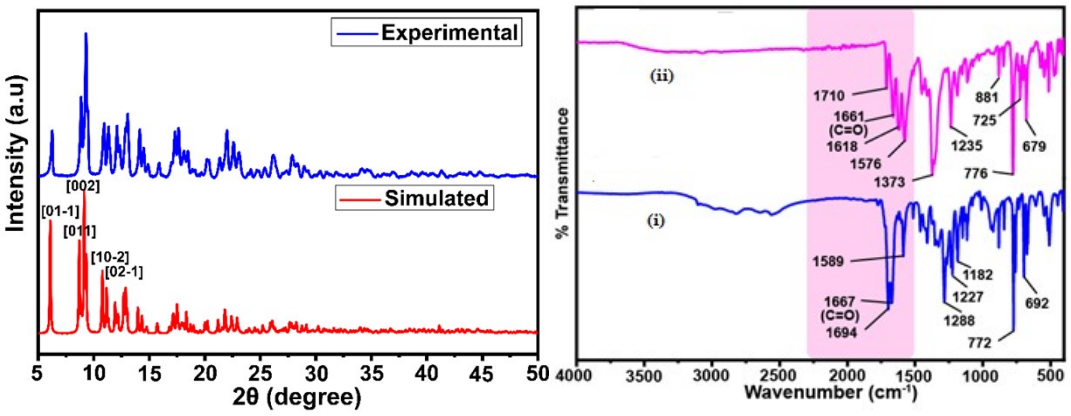

(a) **(b)**

Figure S2: (a) The powder X-ray diffraction pattern of the zinc-coordination polymer (blue): Experimental; (red): simulated from the crystallographic information file; (b) The FT-IR spectra of the (i) **H_2NAPHISO** and (ii) the zinc coordination polymer **Zn_4O-CP**.

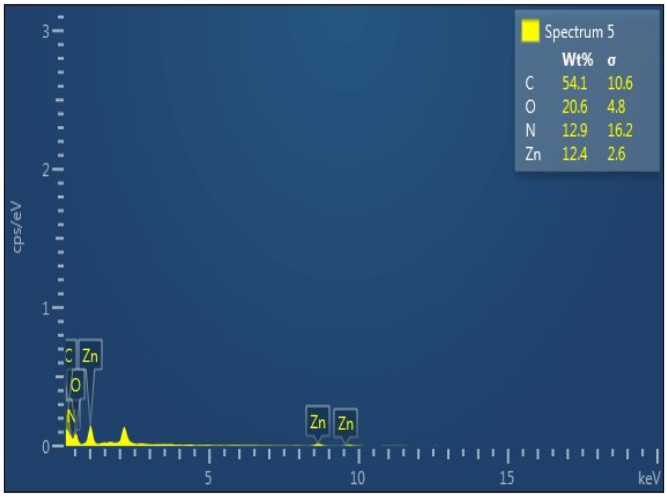

Figure S3: Energy dispersive X-ray (EDX) spectra of powder samples of **Zn_4O-CP.**

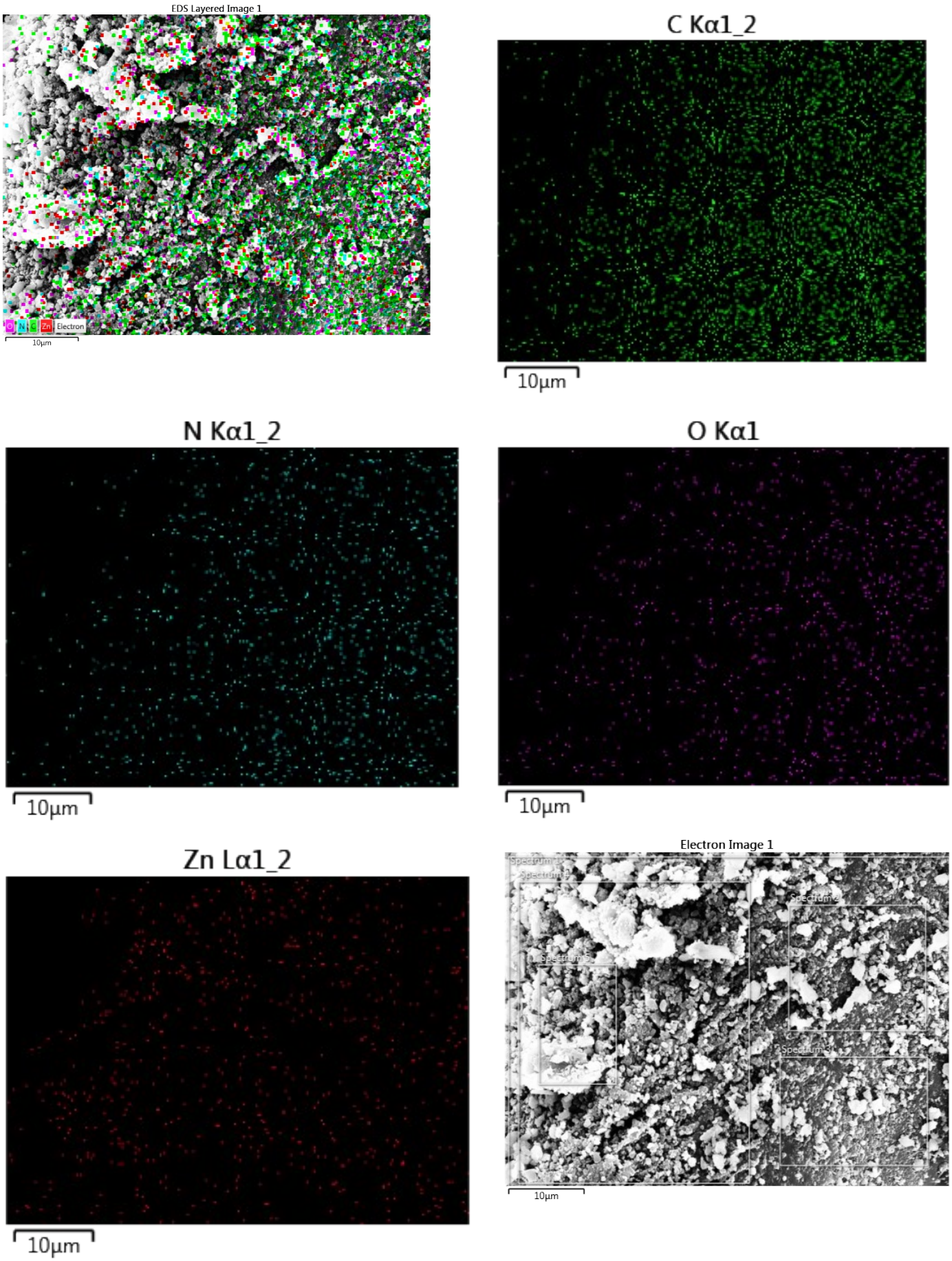

Figure S4: EDX elemental mapping of **Zn_4O-CP**

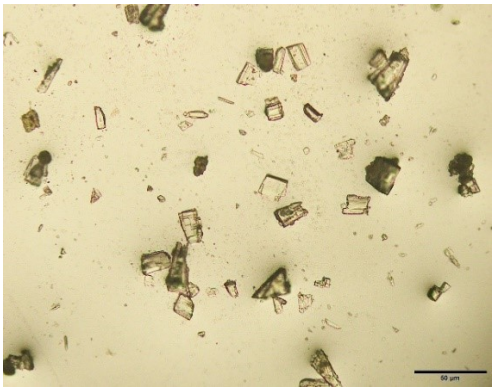

(i)

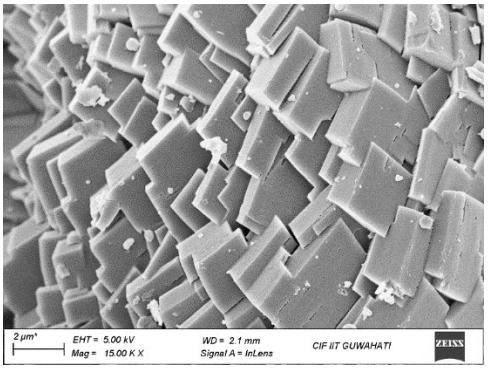

(ii)

Figure S5: (i) The optical microscopic images of the crystals and (ii) SEM images of the powdered samples of the **Zn_4O-CP**.

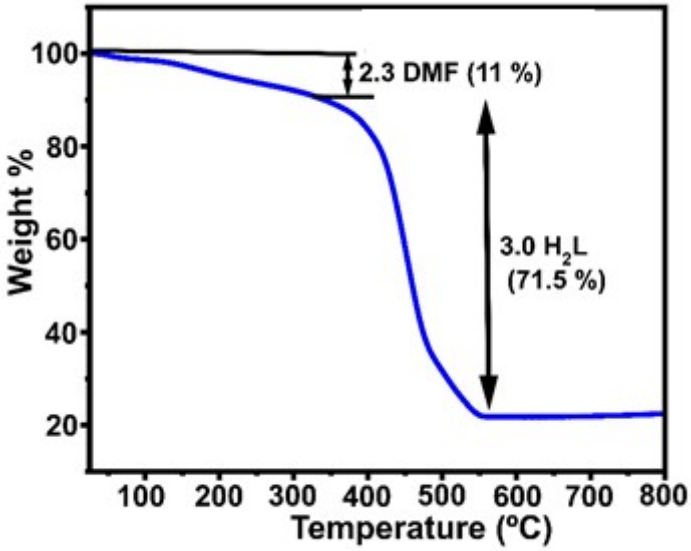

Figure S6: Thermogravimetry of the **Zn_4O-CP** under nitrogen atmosphere at a heating rate of 10 ºC/min.

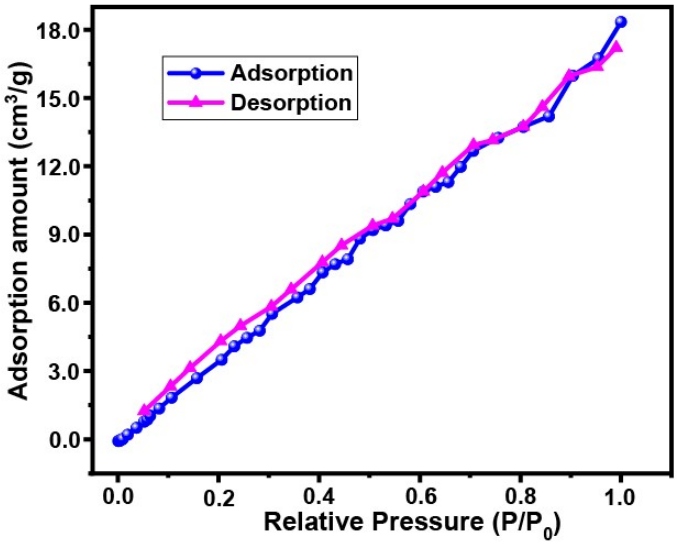

Figure S7: Nitrogen gas adsorption and desorption isotherm of **Zn_4O-CP** performed at -196 °C.

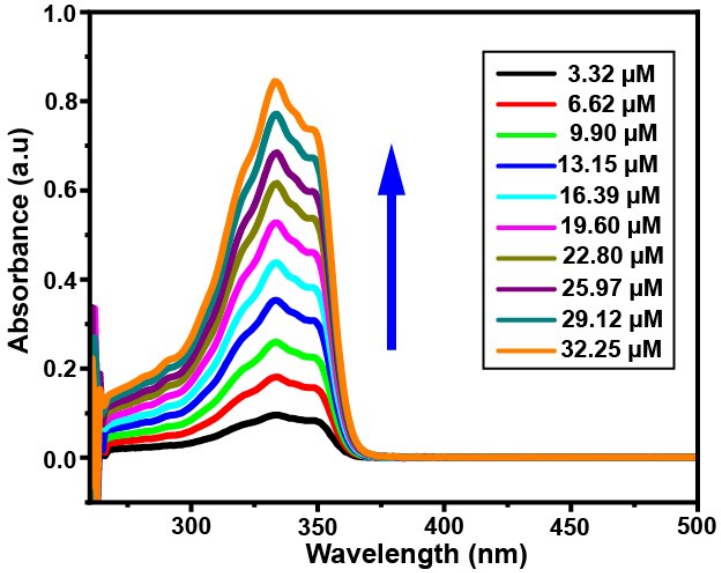

Figure S8: Concentration-dependent UV-visible spectra of **H_2NAPHISO** (λ_{max} = 335 nm) (3 mL, 1 mM of **H_2NAPHISO** in DMF by adding 10 µL in aliquots1 mM of the same).

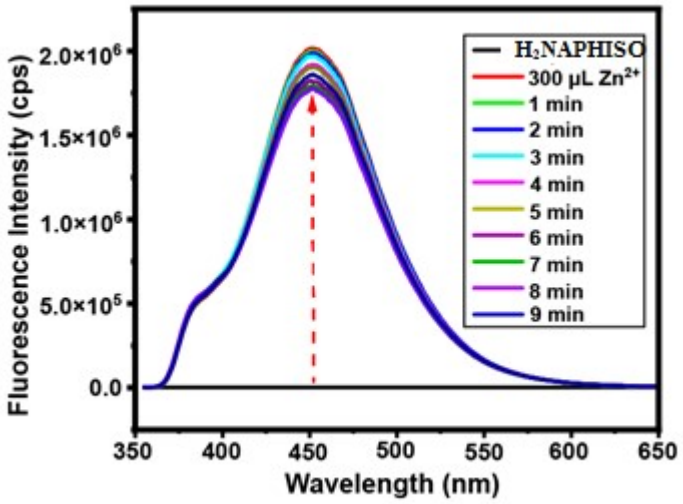

.

Figure S9: Fluorescence emission of **H_2NAPHISO** (1 mM in DMF, 3 mL, λ_{ex} = 335 nm, λ_{em} = 452 nm) with zinc(II) acetate (300 µL 10 mM in water) recorded after one minute for nine times.

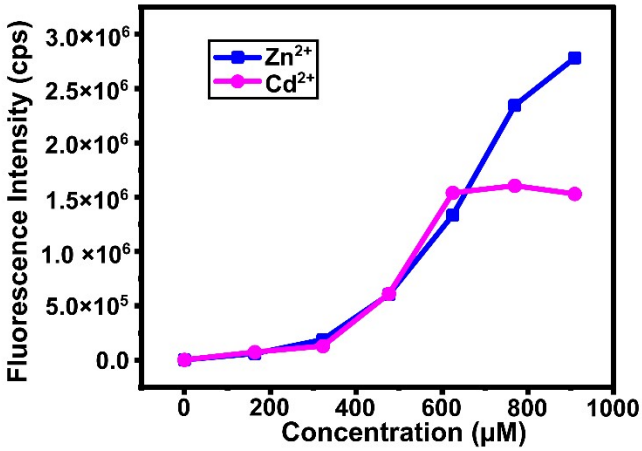

Figure S10: Plots of fluorescence intensity v/s concentration of the solution of the **H_2NAPHISO** (1 mM in DMF, 3 mL) with aqueous Zn^{2+} ions (10 mM) and Cd^{2+} ions (10 mM) at different concentrations.

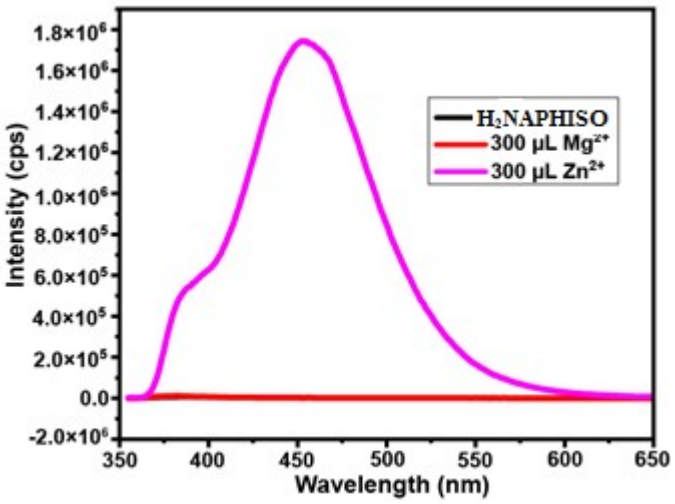
H₂NAPHISO
300 µL Mg²⁺
300 µL Zn²⁺
Intensity (cps)
Wavelength (nm)

(a)

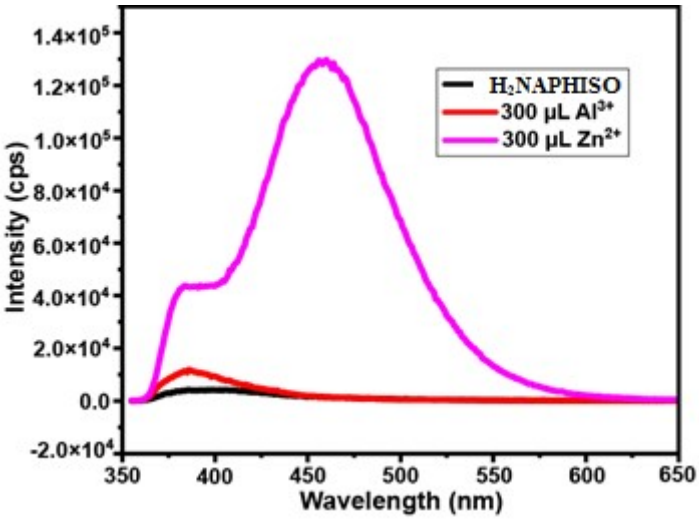
H₂NAPHISO
300 µL Al³⁺
300 µL Zn²⁺
Intensity (cps)
Wavelength (nm)

(b)

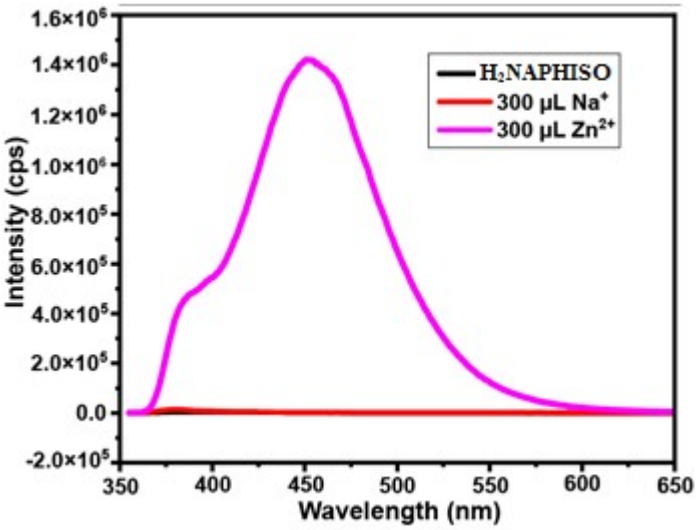
H₂NAPHISO
300 µL Na⁺
300 µL Zn²⁺
Intensity (cps)
Wavelength (nm)

(c)

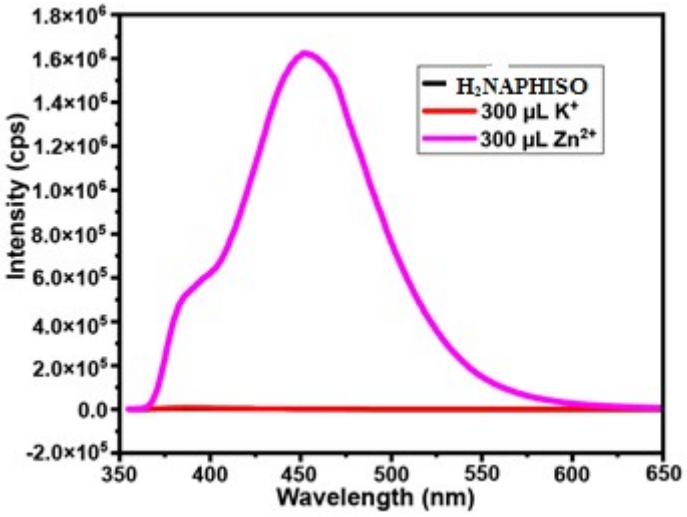
H₂NAPHISO
300 µL K⁺
300 µL Zn²⁺
Intensity (cps)
Wavelength (nm)

(d)

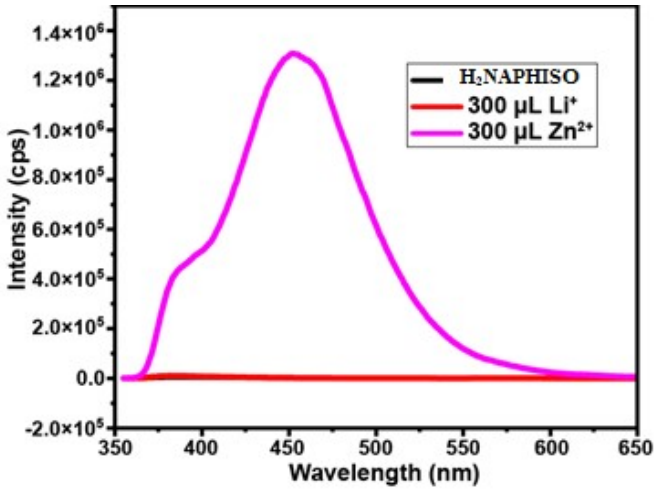
H₂NAPHISO
300 µL Li⁺
300 µL Zn²⁺
Intensity (cps)
Wavelength (nm)

(e)

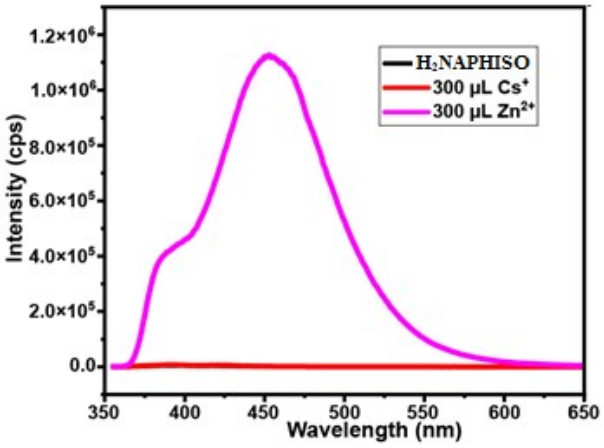
H₂NAPHISO
300 µL Cs⁺
300 µL Zn²⁺
Intensity (cps)
Wavelength (nm)

(f)

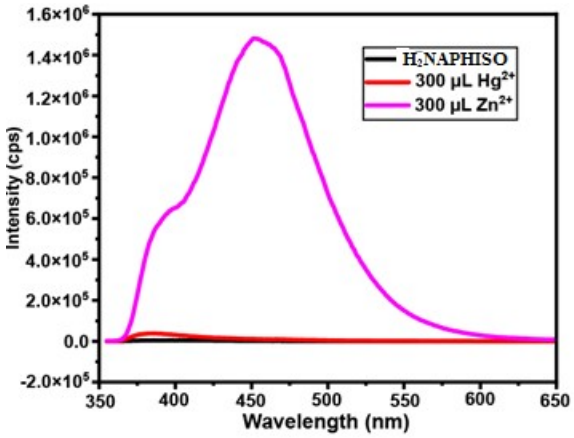
H2NAPHISO
300 µL Hg2+
300 µL Zn2+
Intensity (cps)
Wavelength (nm)

(g)

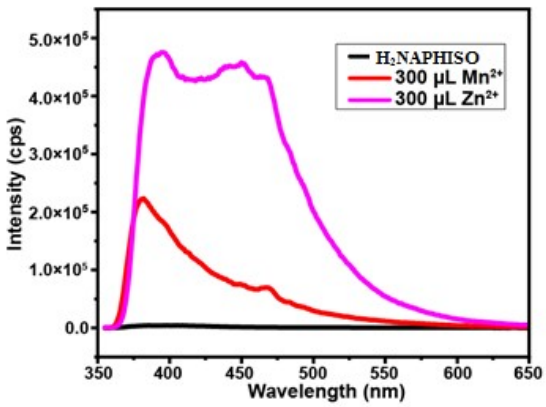
H2NAPHISO
300 µL Mn2+
300 µL Zn2+
Intensity (cps)
Wavelength (nm)

(h)

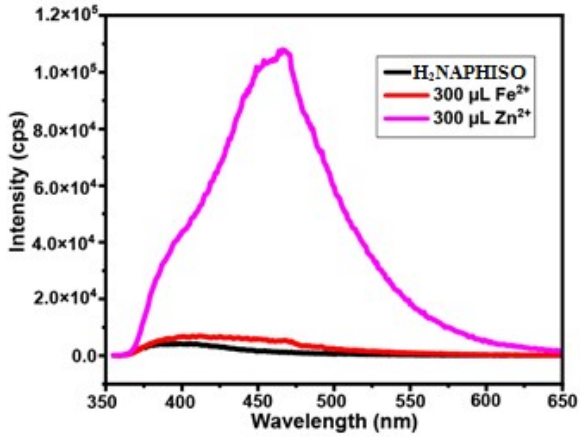
H2NAPHISO
300 µL Fe2+
300 µL Zn2+
Intensity (cps)
Wavelength (nm)

(i)

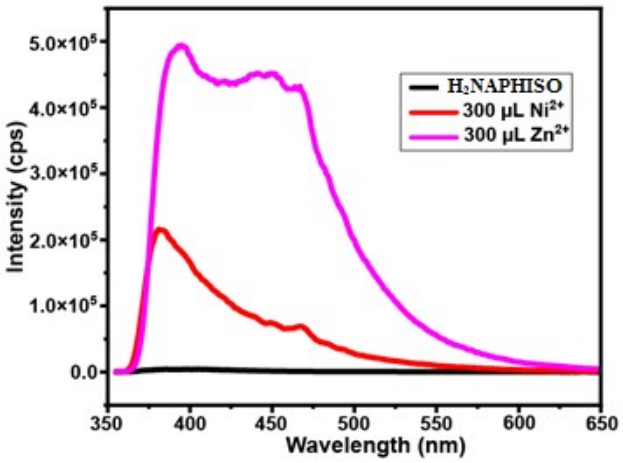
H2NAPHISO
300 µL Ni2+
300 µL Zn2+
Intensity (cps)
Wavelength (nm)

(j)

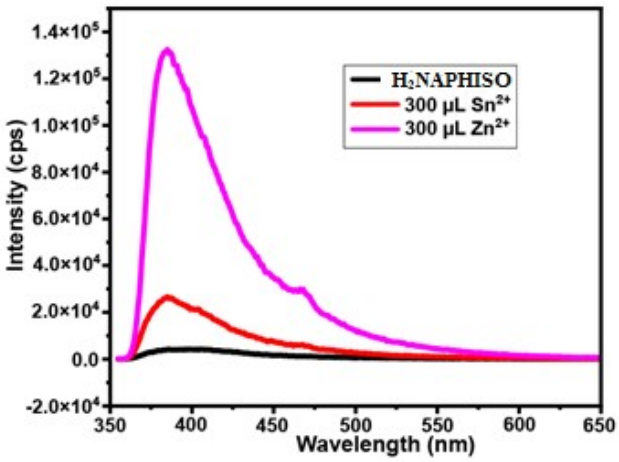
H2NAPHISO
300 µL Sn2+
300 µL Zn2+
Intensity (cps)
Wavelength (nm)

(k)

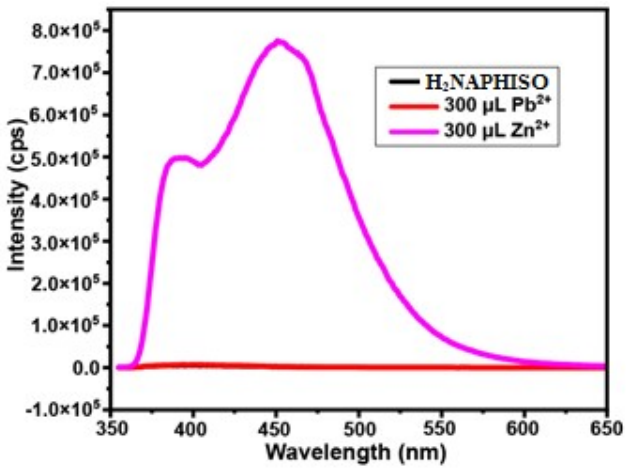
H2NAPHISO
300 µL Pb2+
300 µL Zn2+
Intensity (cps)
Wavelength (nm)

(l)

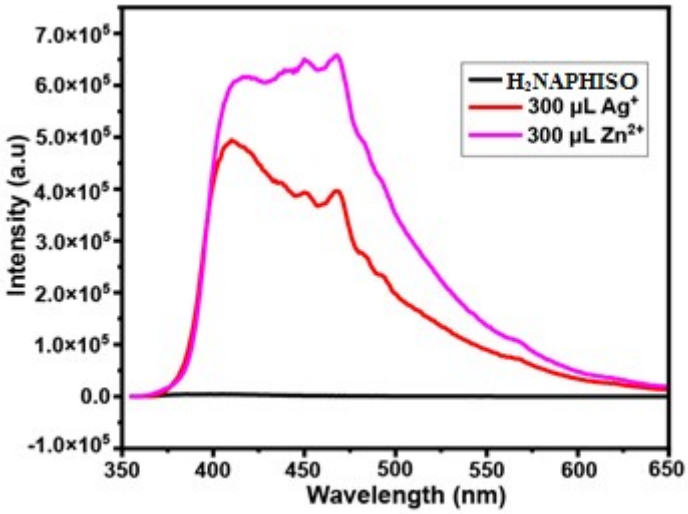

(m)

Figure S11: Fluorescence emission spectra of **H_2NAPHISO** (1mM solution in DMF, 3000 µL taken in cuvette) (λ_{ex} =333 nm, λ_{em} = 452 nm) with aqueous Zn^{2+} (10mM, 400 µL) in the presence of (a) Mg^{2+} (b) Al^{3+} (c) Na^{+} (d) K^{+} (e) Li^{+}, (f) Cs^{+} , (g) Hg^{2+} ,(h) Mn^{2+} , (i) Fe^{2+}, (j) Ni^{2+} , (k) Sn^{2+} , (l) Pb^{2+}, (m) Ag^{+} ions (in each case the to a ligand solution the specific metal ion was added followed by solution of zinc ions)

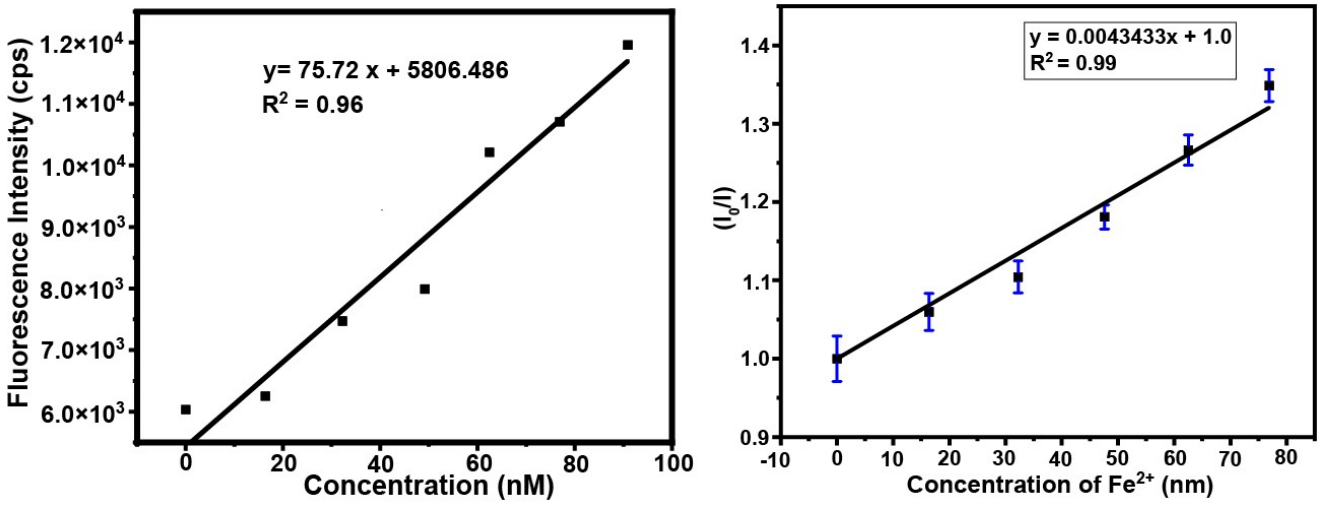

(a) (b)

Figure S12 : Change in the fluorescence emission of (a) **H_2NAPHISO** as a function of concentration of Zn^{2+} ion and (b) Change in I/I_0 of **Zn_4O-CP** with increasing amounts of Fe^{2+} ions.

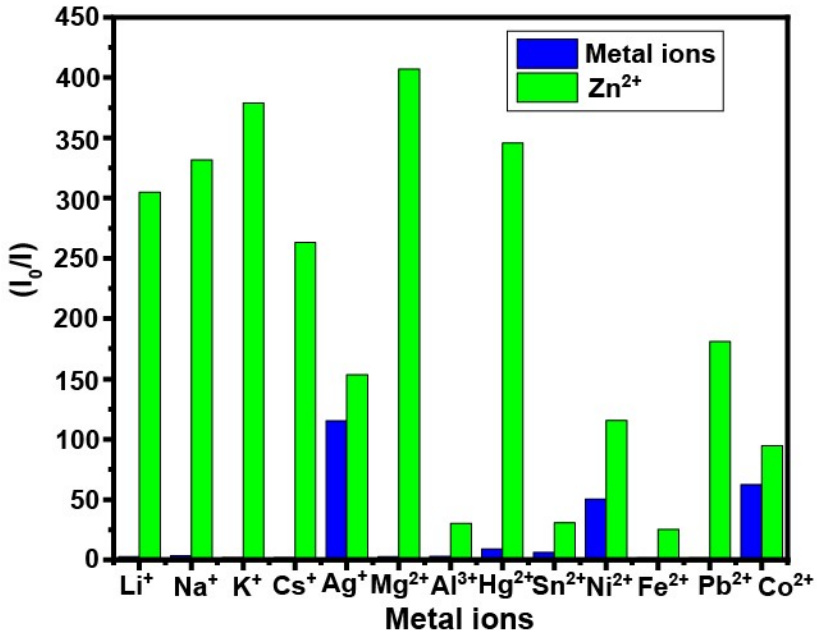

Figure S13: Bar graph of relative changes in the fluorescence emission intensity of **H_2NAPHISO** with different ions with respect to Zn^{2+} ion.

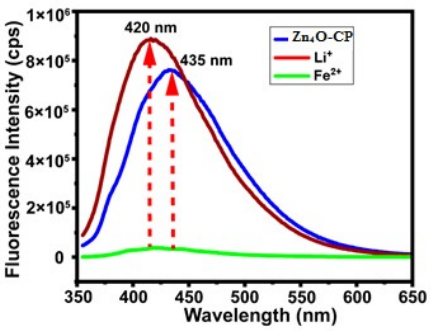

(a)

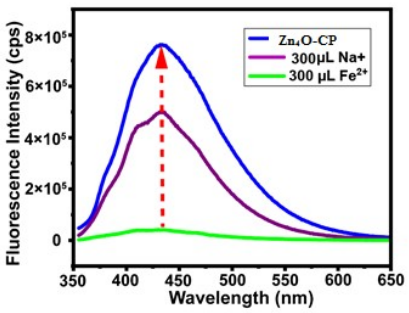

(b)

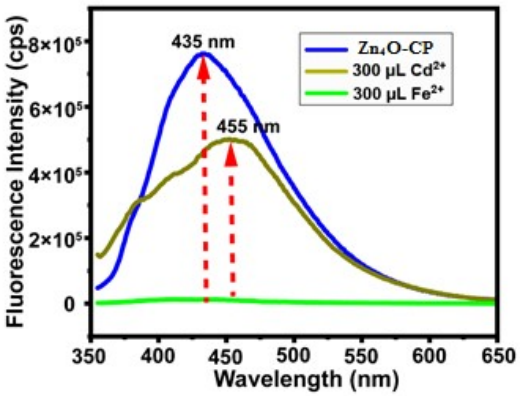

(c)

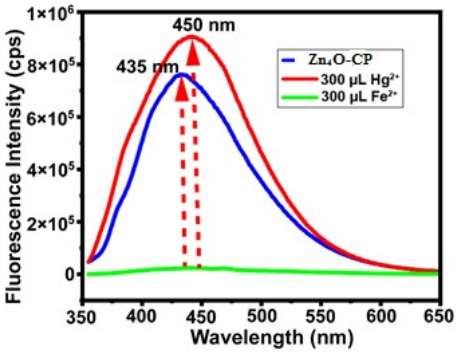

(d)

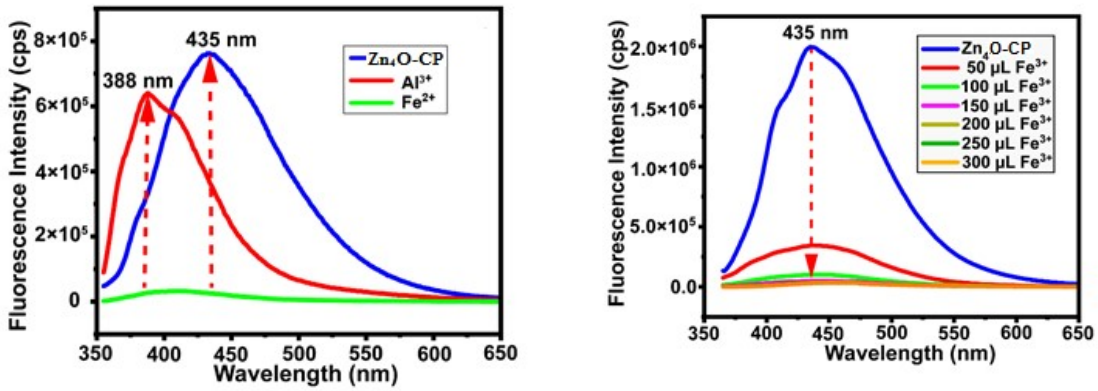

(e) (f)

Figure S14: Competitive fluorescence emission spectra of **Zn_4O-CP** (3mL, 4 mg in 10 mL of DMF with aqueous Fe^{2+} (10mM, 400 µL) in the presence of (a) Li^+ (b) Al^{3+} (c) Cd^{2+} (d) Hg^{2+} (e) Na^+ ions. (f) The emission intensity of Zn_4MOF decreased with the incremental addition of 10 mM aqueous Fe^{3+} solution, ranging from 0 µL to 300 µL (λex = 350 nm, and λem = 435 nm).

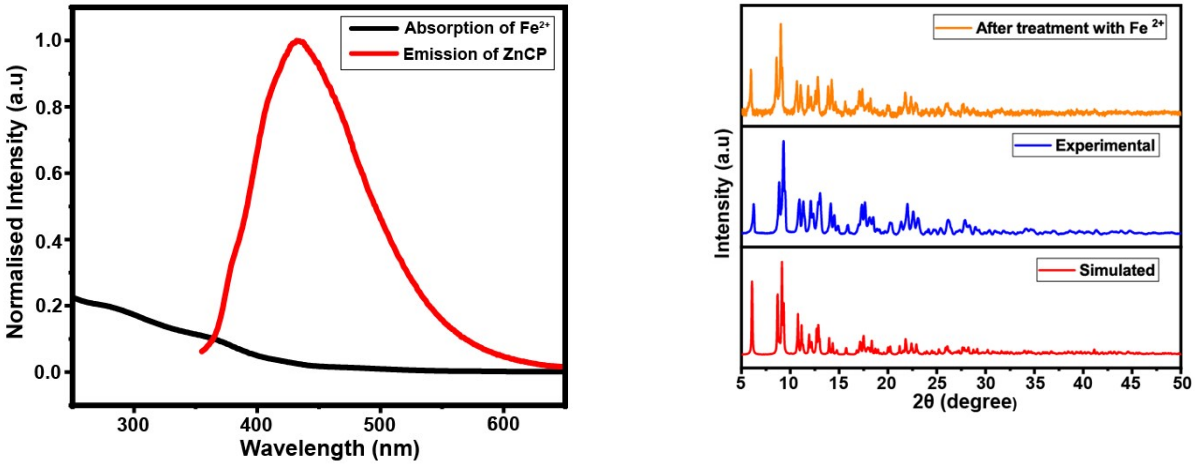

(a) (b)

Figure S15: (a) The absorption and emission spectra of **Zn_4O-CP** in DMF and (b) Comparison of experimental PXRD patterns of the **Zn_4O-CP** and PXRD of the sample after treatment with Fe^{2+}.

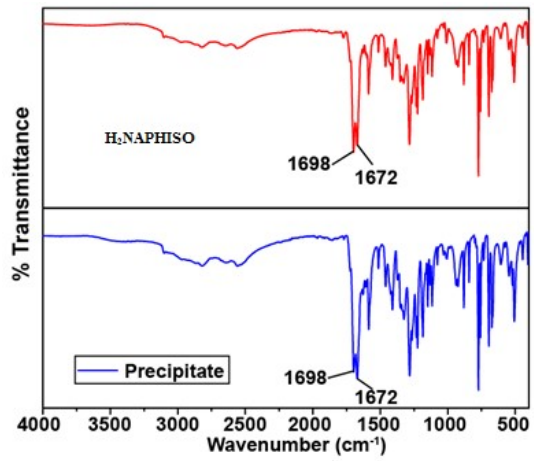

Figure S16: FT-IR spectra of **H_2NAPHISO** and precipitate obtained after treating it with zinc acetate hexahydrate for 2 hrs in DMF at room temperature.

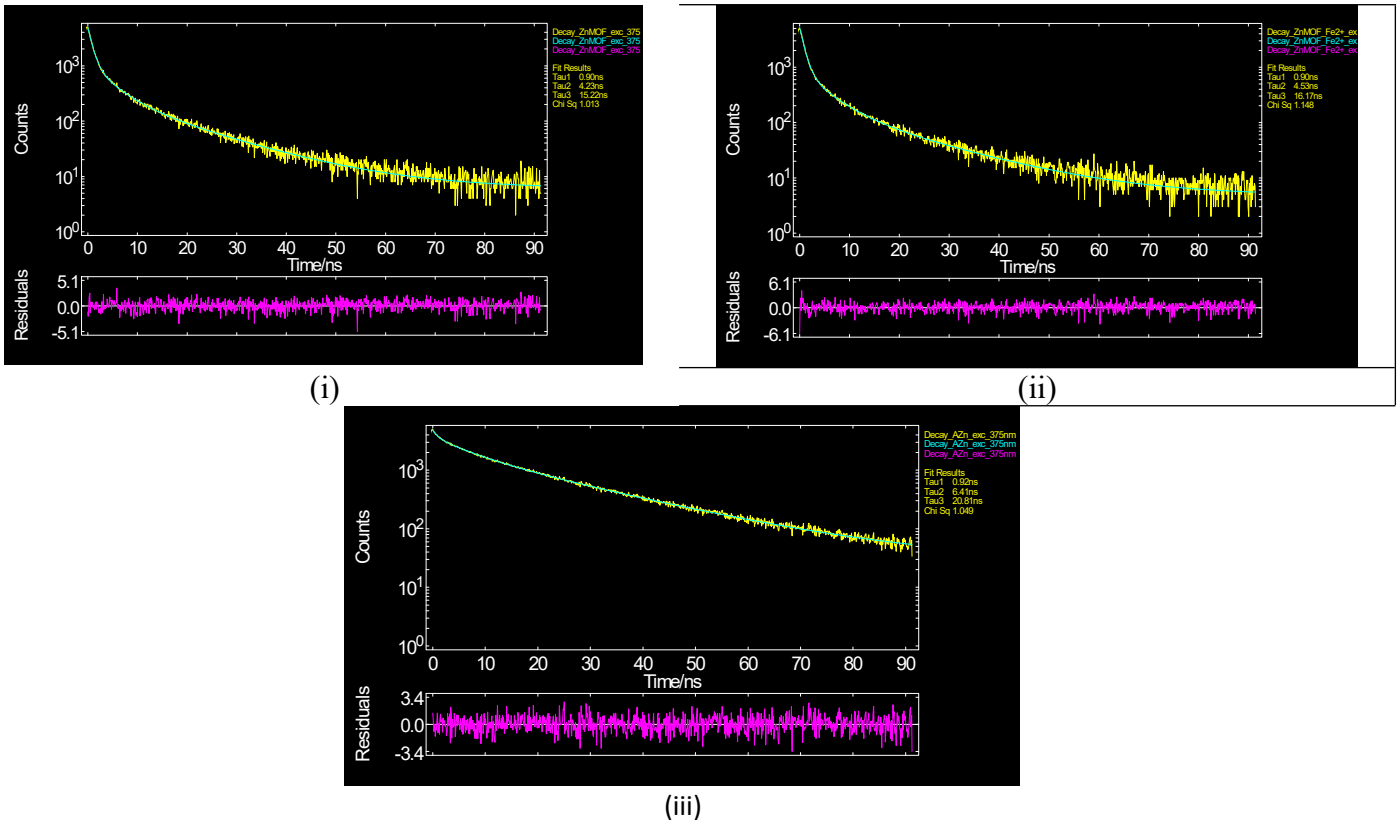

Figure S17: Life-time decay profile of (i) **Zn_4O-CP** (4 mg in 3 mL DMF dispersed by sonication), (ii) by adding Fe^{2+} (200 µL from 10 mM solution in DMF), and (iii) **H_2NAPHISO** (1mM in 3 mL DMF) with 300 µL Zn^{2+} (10 mM stock solution in DMF).

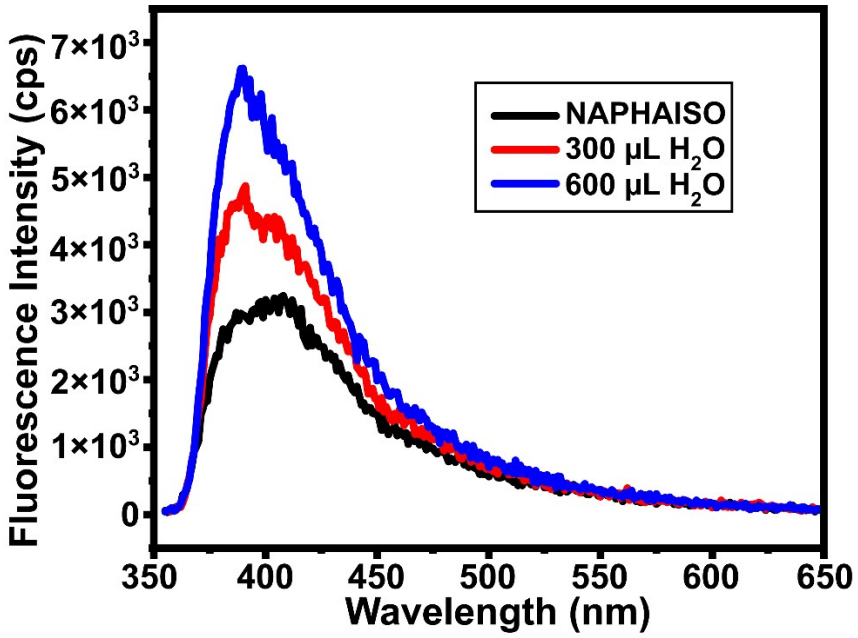

Figure S18: The change in emission spectra of **H_2NAPHISO** (1 mM in DMF, 2.5 mL) incrementally diluted with water

Table S1: Crystals parameters of the Zn_4O-CP

Empirical Formula	$C_{66}H_{48}N_5O_{24}Zn_4$
Formula Weight	1556.57

Space group	Triclinic $P\bar{1}$
a/ Å	10.3826 (6)
b/Å	16.2352 (10)
c/ Å	21.2335 (14)
α/ °	106.864 (2)
β/ °	102.927 (2)
γ/ °	102.216 (2)
V/ Å^3	3188.4 (3)
Z	2
ρ_{cal} (gcm^{-3})	1.621
μ (mm^{-1})	1.575
F(000)	1582
Refl Collected	76522
Independent Refl	11228
Ranges (h, k, l)	-12 ≤ h ≤ 12 -19 ≤ k ≤ 19 -25 ≤ l ≤ 25
Max θ (degree)	25.0
Data/Restraints/Parameter	11228/0/869
GooF (F^2)	1.070
R indexes	0.0507
[I > 2σ]	0.0729
WR_2	0.1284

Table S2: Life-time decay data

Compound	τ_1 (ns) [% fraction]	τ_2 (ns) [% fraction]	τ_3 (ns) [% fraction]	< τ > (ns)	χ^2
Zn_4O-CP	0.8959 [32.72]	4.226 [30.15]	15.22 [37.13]	7.219	1.0129
Zn_4O-CP with Fe^{2+} ions	0.8999 [39.87]	4.533 [29.59]	16.17 [30.54]	6.639	1.1482
H_2NAPHISO with Zn^{2+} ions	0.9220 [2.06]	6.407 [19.40]	20.81 [78.54]	11.129	1.0485

Equation for tri-exponential fit: $A + B_1\exp(-t/\tau_1) + B_2\exp(-t/\tau_2) + B_3\exp(-t/\tau_3)$

$< \tau > = (B_1\tau_1^2 + B_2\tau_2^2 + B_3\tau_3^2)/(B_1\tau_1 + B_2\tau_2 + B_3\tau_3)$

Table S3: Comparison on the detection limit of various substrates reported recently for Fe^{2+} ions

Compound/composite	Detection limit	Reference
Phenanthroline derivative	2.60 ppb	H. Nawaz, W. Tian, J. Zhang, R. Jia, Z. Chen, J. Zhang, *ACS Appl. Mater. Interfaces.* 2018, *10*, 2114 - 2121.
Eu-MOF	2.00 nM	Y. Cheng, M. Wu, Z. Du, Y. Chen, L. Zhao, Z. Zhu, X. Yu, Y. Yang, C. Zeng,. *ACS Appl. Mater. Interfaces.* 2023, *15*, 24570 - 24582.
2-((3-Hydroxyphenyl)amino)-3-(phenylthio)naphthalene-1,4-dione	0.27 μM	P. Ravichandiran, A. Boguszewska-Czubara, M. Masłyk, A. P. Bella, S. A. Subramaniyan, P. M. Johnson, K. S. Shim, H. G. Kim, D. Yoo,
Polyoxometalate	8.00 nM	Y. Xu, P. Li, X. Hu, H. Chen, Y. Tang, Y. Zhu, X. Zhu, Y. Zhang, M. Liu, S. Yao, *ACS Appl. Nano Mater.* 2021, *4*, 8302 - 8313.
Naphthalimide derivative	82.00 nM	T. Yan, X. Wang, C. Liu, X. Cai, Y. Wang, X. Liu, X. Rong, K. Wang, W. Li, W.
Carbamoyl oxime		Sheng, B. Zhu, *J. Agricultural and Food Chem.* 2024, *72* , 13341 - 13347
Naphthalimide derivative	0.50 μM	W. Xuan, , R. Pan, Y. Wei, Y. Cao, H. Li, F.-S. Liang, K.-J. Liu, J. B. Wang,

		Bioconjugate Chem. 2016, *27*, 302 - 308.
S–S derivative	17.54 nM	D. C. Immanuel, N. Bhuvanesh, H. Jayaraj, A. Thamilselvan, D. P. Devi, A. Abiram, J. Prabhu, R. J. A. O. Nandhakumar, *ACS Omega.* 2020, *5*, 3055 - 3072.
CdTe quantum dot	5.00 nM	P. Wu, Y. Li, X.-P. J. A. Yan, *Anal. Chem.* 2009, *81* , 6252 - 6257.
Salicylyliminedibenzyl derivative	3.96 ppb	R. Joseph, J. P. Chinta, C. P. Rao, *Inorg. Chem.* 2011, *50* , 7050 - 7058.
ZnO_4-CP	42.57 nM	This work